High gain and circularly polarized substrate integrated waveguide cavity antenna array based on metasurface

Hao Bai(白昊), Guang-Ming Wang(王光明)†, and Xiao-Jun Zou(邹晓鋆)

Air and Missile Defend College, Air Force Engineering University of China, Xi'an 710051, *China*

(Received 11 February 2022; revised manuscript received 24 April 2022; accepted manuscript online 28 April 2022)

Two substrate integrated waveguide (SIW) cavity antenna arrays based on metasurface are proposed in this paper. By rotating the metasurface element, circularly polarized and high gain antennas are achieved respectively. Firstly, multi-mode resonance theory is employed to broaden the bandwidth of the slot antenna. And then, an SIW cavity composed of 4×4 cornercut elements is added on the top of the slot antenna to achieve the circular polarization and improve the front-to-back ratio. Thirdly, the metasurface elements are sequentially rotated and a high gain antenna with 2-dBi enhancement on average in the operation band is obtained. Based on the two antenna units, two 2×2 antenna arrays are designed. The circularly polarized and high gain antenna arrays are both fabricated to verify the correctness. Furthermore, the novel wideband phase shifter is employed in the circularly polarized antenna to obtain an operating bandwidth of 38% (4.05 GHz–5.95 GHz) and AR bandwidth of 24.9% (4.4 GHz–5.65 GHz). The bandwidth of the high gain antenna can reach 42.7% (3.95 GHz–6.1 GHz) and with the gain enhancement of 2 dBi compared with that of the circularly polarized antenna. The gain remains steady in most of operating band within a variation of 1 dBi. It is remarkable that the rotating of the metasurface element has a great influence on the antenna performance, which provides a new explication for the multi-function antenna design.

Keywords: substrate integrated waveguide (SIW), cavity antenna, metasurface, high gain, circularly polarized

PACS: 41.20.Jb, 73.20.Mf **DOI:** 10.1088/1674-1056/ac6b22

1. Introduction

As the terminal of communications system, antenna plays an important part in the whole system. The detection distance represents the performance of antenna. For an antenna, the detection distance and accuracy are reflected in the gain of the antenna.[1–4] The higher the gain, the longer the detection range is. High gain antennas have been studied extensively. A metasurface high gain antenna is proposed in Ref. [5]. The array designed for wideband operation and high gain has achieved an impedance bandwidth 31% with a peak gain of 14.5 dBi. In Ref. [6], a hybrid metasurface broadband array is proposed. In all operating band, the impedance bandwidth is 28%, meanwhile the peak gain is 8.4 dBi. On the other hand, compared with linearly polarized counterparts, the circularly polarized antennas are favorable in wireless communications on account of its capability of mitigating multipath fading.[7–10] How to broaden the circularly polarized bandwidth and realize the broadband circularly polarized antenna is a difficult problem. The presence of sequential rotation provides a new idea to achieve the broadband circularly polarized antenna.[11–13] A broadband circularly polarized (CP) antenna array fed by a sequential-phase (SP) network is proposed in Ref. [11]. In Ref. [12], a Ka-band CP array antenna with high efficiency and wide axial ratio (AR) bandwidth is designed. It has 21.2% AR bandwidth and maintains stable gain in the operating band.

The SIW antennas are frequently employed in modern antenna design due to their high Q value and easy integration.[14] Also the low-profile cavity-backed slot antennas based on SIW technology have received a lot of attention.[15,16] The backed cavities and feeding elements of this antenna can be completely constructed at a single substrate. And the antenna has the advantage of high radiation performance, low-profile, low-cost fabrication, and seamlessly planar integration.[17,18] In Ref. [19], a broadband 4-unit cavity-backed slot array based on SIW is demonstrated. This antenna adopts unit stack and multi-feed technology to obtain a wide operating bandwidth. Good radiation performance is obtained in the working band. As the new developed technology, metasurface has received the attention of researchers recently.[20,21] Metasurface is employed to improve the antenna performance, such as broadening the bandwidth,[22,23] beam controlling,[24] polarization transformation,[25] and gain enhancement.[26] In Ref. [27], a metasurface multilayer wideband CP antenna array is proposed for Q-band applications. The antenna array has reached 32% of S_{11} bandwidth, 25.8% of 3-dB AR bandwidth, and 27.6% of 3-dB gain bandwidth, and 18.2-dBic peak gain. In Ref. [28], the complemental boundaries is introduced for the first time into the periodic metasurface antenna, further enlarging the effective aperture of radiation and increasing the gain by about 1.5 dB through new technical improvements.

In this work, a high gain and circularly polarized substrate integrated waveguide (SIW) cavity antenna array is proposed. And both of the arrays are designed based on metasurface. By rotating the metasurface element, two arrays are

†Corresponding author. E-mail: wgming01@sina.com

© 2023 Chinese Physical Society and IOP Publishing Ltd

achieved respectively. To verify the design, both the circularly polarized antenna array and the high gain antenna array are fabricated and measured. The operating bandwidth and the AR bandwidth of the circularly polarized array are 38% (4.05 GHz–5.95 GHz) and 24.9% (4.4 GHz–5.65 GHz) respectively. The bandwidth of the high gain antenna can reach 42.7% (3.95 GHz–6.1 GHz) and the gain enhancement of 2 dBi compared with the counterpart of the circularly polarized antenna. The gain of 1 dBi remains steady in most of the working bands. We can see that the rotation of the metasurface element has a great influence on the antenna performance which can be widely used in the antenna design.

2. Antenna unit configuration and results

2.1. Structure of sub-array

The structure of the proposed high gain antenna sub array, which is made up of three-layer metal patches and two-layer substrates, is shown in Fig. 1. The metasurface is etched on the upper layer of the 3-mm-thick top substrate. The ground with slot is printed on both layers of the 0.8-mm-thick bottom substrate. The metal vias with spacing $P_{\rm siw}$ and diameter of $D_{\rm siw}$ are constructed to connect the ground and patches. The feeding network is on the lower layer of the bottom substrate. All substrates are of Rogers 4003C with the relative permittivity of 3.38. From Fig. 1, we can see that the antenna unit is fed by the multi-mode slot antenna, which is a common and classic method to broaden the bandwidth used by some researchers.[29] Two short horizontal lines with uniform gaps are symmetrically added near zero. Additional radiation modes are introduced. Then, broadband slot antenna with two resonances is obtained by combining full-wavelengths provided by the first slot. Metasurface is added on the top of the radiation antenna to further improve the antenna performance.

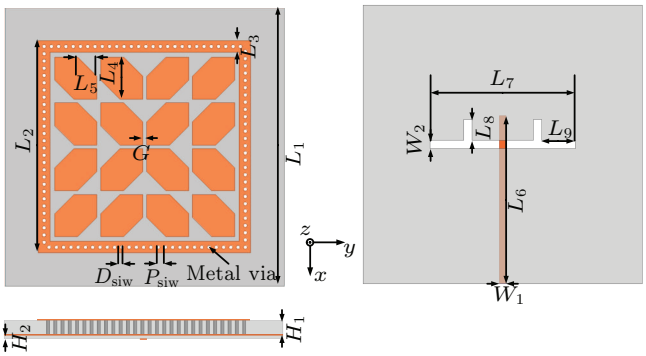


Fig. 1. Structure of proposed high gain antenna sub array, with dimensions being $L_1 = 73$, $L_2 = 55$, $L_3 = 3$, $L_4 = 11$, $L_5 = 4.5$, $L_6 = 44$, $L_7 = 38$, $L_8 = 5.4$, $L_9 = 8.8$, $W_1 = 1.8$, $W_2 = 2.2$, $g = 1$, $D_{\rm siw} = 1$, $P_{\rm siw} = 1.9$, $H_1 = 3$, and $H_2 = 0.8$, and all in unit: millimeters.

On the other hand, the front-to-back ratio of the traditional slot antenna is small, which means more energy loss. In this work, the SIW cavity is employed to enhance the front-to-back ratio. Above all, the gain of the antenna is improved by 2-dBi enhancement through optimizing the metasurface element. To illustrate the effect of metasurfaces on the sub array, figure 2 gives the difference between the antenna performance with and without the metasurfaces. By loading the metasurface, the bandwidth is increased by 10.1% and the gain is improved by a maximum value of 3dBi, proving the necessity of introducing the metasurface in the antenna unit.

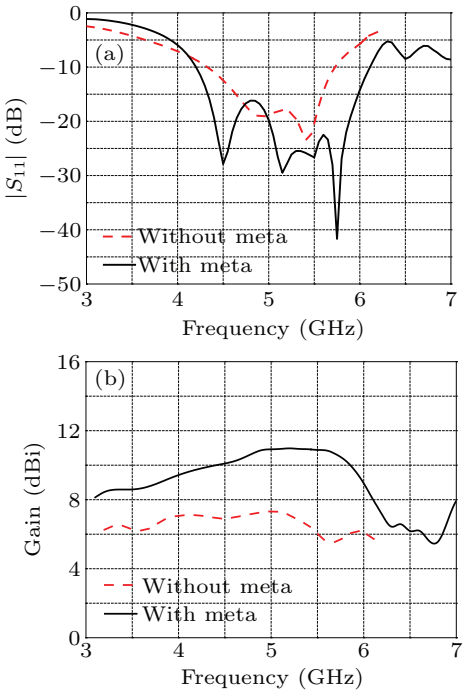


Fig. 2. Comparison of (a) *S*-parameter and (b) gain between antenna with and without metasurface.

2.2. Evolution of sub array

To further analyze the design solution of the antenna, the evolution of the sub array is given in Fig. 3. It is apparent from Fig. 3 that the antenna (Ant.) is made up of two-layer substrates and fed by the multi-mode slot antenna. Metasurface consists of 4×4 corner-cut elements which is on the top of the first layer substrate. Based on Ant. 1, the SIW cavity is introduced at the metasurface periphery to form Ant. 2. And then, the metasurface element of Ant. 1 is modified by rotating the elements located in the first and third quadrant by 180°, and optimizing the corner-cut size. In the same way, Ant. 3 is formed. Finally, on the basis of Ant. 3, the SIW cavity is introduced at the metasurface periphery to form Ant. 4 which is the designed antenna sub-array.

Figure 4 plots the comparisons of index among Ant. 1 to Ant. 4. It is evident that the operating band increases from 1.5 GHz (4.15 GHz–5.65 GHz) of Ant. 1 to 1.7 GHz (4.3 GHz–6 GHz) of Ant. 3.

By optimizing the metasurface element, the bandwidth increases by 200 MHz (4%). Meanwhile, the gain of Ant. 3 is enhanced to a certain extent compared with that of Ant. 1 in the whole working band, with a minimum gain improvement of 1.29 dBi (4.6 GHz) and a maximum one of 2.2 dBi

(5.5 GHz), which is displayed in Fig. 4(c). At 5 GHz, the gain on the broadside (Z axis) is increased by 1.9 dBi as shown in Fig. 4(d). By introducing SIW cavity into Ant. 1 and Ant. 3, Ant. 2 and Ant. 4 are achieved respectively. We can see that the impedance bandwidths of the two antennas are both enhanced in this lower frequency band, with enhancement of 200 MHz and 100 MHz, respectively. Meanwhile, the gain is improved by 0.4 dBi and the axial ratio is virtually unaffected. This means that the SIW cavity will not have a negative effect on the original antenna. From Fig. 4(d), it can be clearly seen that the SIW cavity can reduce the backward radiation effectively and improve the front-to-back ratio. Owing to the SIW cavity's constraint of energy, the energy loss is reduced and the gain is improved to some degree. Simultaneously, the backward radiation is reduced due to the radiation characteristic of the SIW cavity itself. Thus, the front-to-back ratio is improved. Significantly, first, the classical corner-cut element is employed by Ant. 1 and Ant. 2 to obtain the circular polarization. But the bandwidth is only 350 MHz (4.55 GHz–4.9 GHz) and is very narrow. To further improve the bandwidth, the classical rotation of feed network is introduced which will enhance the availability. Second, although the gain is stable in the most working band, which can be seen from Fig. 4(c), a drop disappears in the higher band. Take the Ant. 4 for example, the variation of the gain is 1.1 dBi in the band from 4.3 GHz to 5.9 GHz, while 2 dBi in the higher part from 5.9 GHz to 6.1 GHz. On the whole, the entire operation band satisfies the 3-dB gain bandwidth and is highly practicable. How to improve the gain in the higher band is the key research content of the next step.

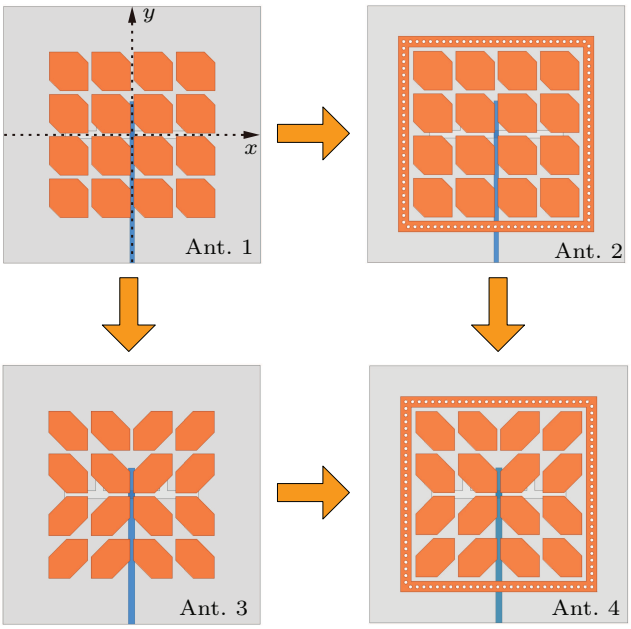


Fig. 3. Evolution of the sub array.

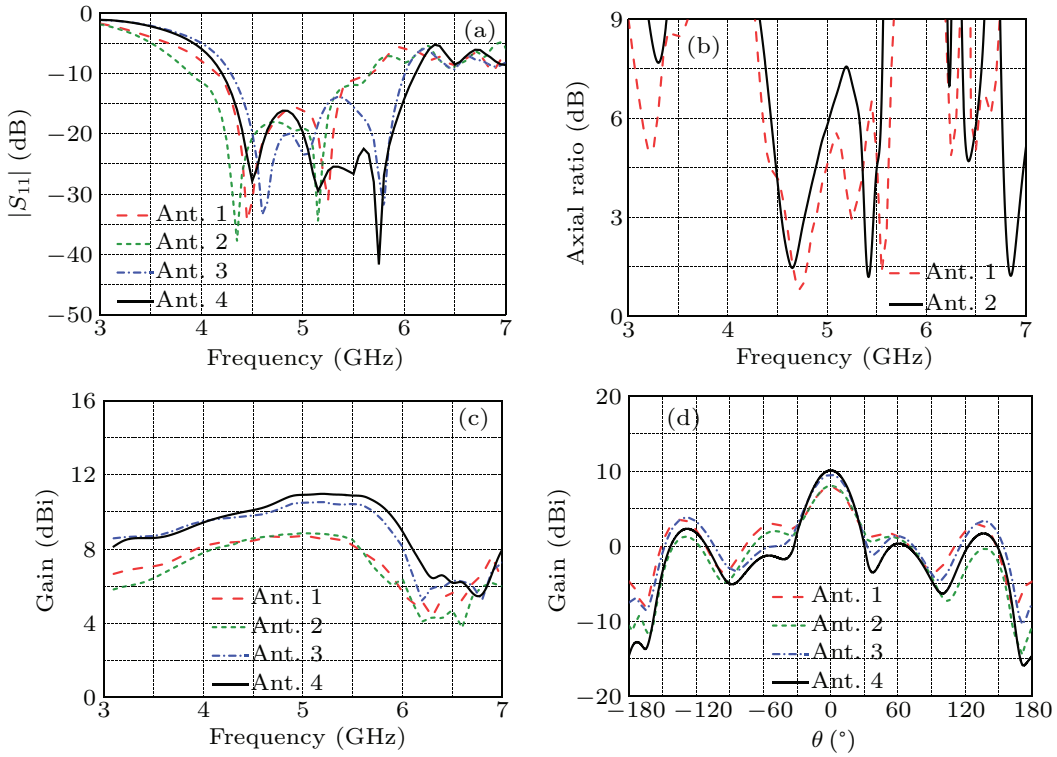


Fig. 4. Comparisons of index among Ant. 1 to Ant. 4.

2.3. Analysis of current distribution

Comparisons between the current diagrams (5 GHz) in some elements of Ant. 1 and Ant. 3 are demonstrated in Fig. 5 to further explain the principle of improving the gain by modifying the metasurface. For Ant. 1, the direction of the current in the same phase is almost the same due to the identical 4×4

elements. If the 8 elements in the first quadrant and the third quadrant are rotated 180° as shown in Fig. 5(b), the direction of the current in the first quadrant and the third quadrant will change with the rotation while the second quadrant and the fourth quadrant do not change. It can be clearly seen that the direction of the current changes obviously and the current intensity increases with the superposition that leads the radiation energy to improve. Thus, the gain is improved.

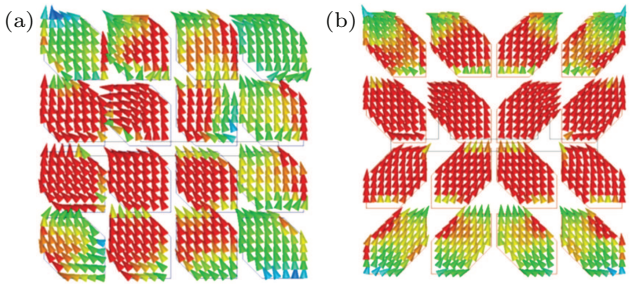


Fig. 5. Comparison of current diagram (5 GHz) among some elements in (a) Ant. 1 and (b) Ant. 3.

3. Study and discussion of antenna array

3.1. Design of antenna array

Based on Ant. 2 and Ant. 4, array 1 and array 2 are obtained respectively as shown in Fig. 6. Figure 6(a) exhibits the extended diagram of the proposed circularly polarized array which consists of two layers of substrates and three layers of metal patches. The blue part is the feed network. The distance between the elements is D and the whole dimension is 143 mm×143 mm×3.8 mm.

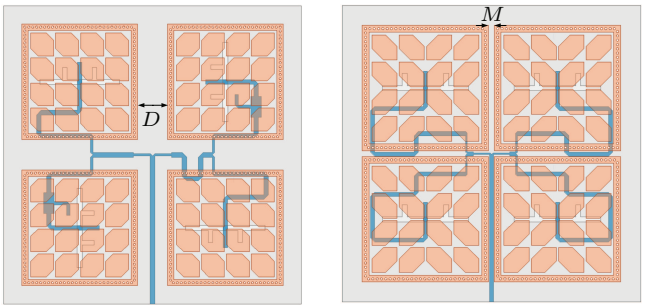


Fig. 6. Structure of the proposed array 1 and array 2 (D = 15 mm, M = 2.5 mm).

The four sub-arrays are placed in order to improve the AR bandwidth and are fed by the network shown in Fig. 7. The configuration of the feed network and the novel wideband phase shifter and the detailed description of each part are given in Fig. 7. By adjusting the width of the phase shifter W_3, the length of the branch L_{11} and L_{12}, the phase control will be achieved in the broad operating band. The curve of frequency dependent S parameter of the phase shifter and the curve of frequency dependent phase variation are displayed in Fig. 8, from which we can see that the phase difference is 90° ± 3.5° in the entire operating band. The high gain antenna array of the similar structure with unit is displayed in Fig. 6(b). The array has a size of 131 mm×134 mm×3.8 mm with the unit spacing of M. The SIW cavity has the great ability to restrain the energy leakage and the coupling between the adjacent units is small which has been verified by other researchers.[15] Thus, the spacing M is chosen to be as small as possible to reduce the size and achieve miniaturization. The blue part is feed network composed of traditional one in four constant-amplitude same-phase power divider. This design is simple which provides a great availability in the practical application.

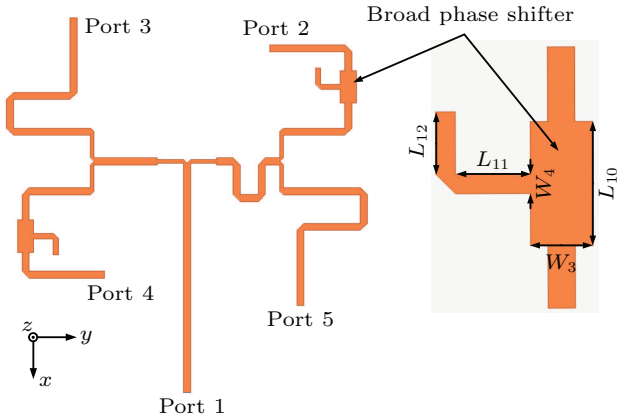


Fig. 7. Feed network of CP antenna array.

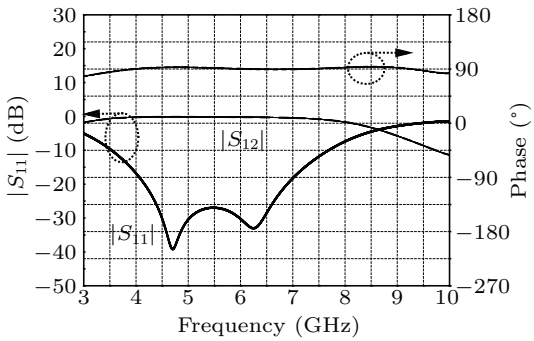


Fig. 8. Frequency-dependent S parameter of phase shifter and phase.

3.2. Measurement and discussion

The circularly polarized and high gain antenna array is fabricated to verify the design correctness. The two photographs of the arrays are displayed in Fig. 9. The S-parameters and radiation characteristics of the arrays are respectively measured by an AV 3672B vector network analyzer and in the anechoic chamber. Figure 10 demonstrates the photographs of the measurement environment. The measured and simulated S parameters of the antenna arrays are shown in Fig. 11. We can see that the simulated operating band of the high gain array is 2.15 GHz (3.95 GHz–6.1 GHz) while the measured one is 2.1 GHz (4 GHz–6.1 GHz). And the simulated operating band of the CP array is 1.9 GHz (4.05 GHz–5.95 GHz) while the measured one is 1.8 GHz (4.15 GHz–5.95 GHz). The difference between the simulated and measured results originate from the machining error and welding quality. We note that

the bandwidths of the two antenna arrays are improved compared with the *S* parameter of the corresponding units. This is attributed to the feed network, especially the feed network of the circularly polarized which has obvious effect on broadening the bandwidth.

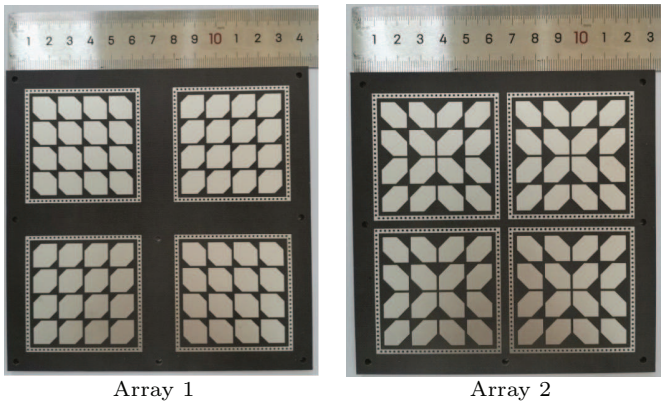


Fig. 9. Photographs of antenna arrays.

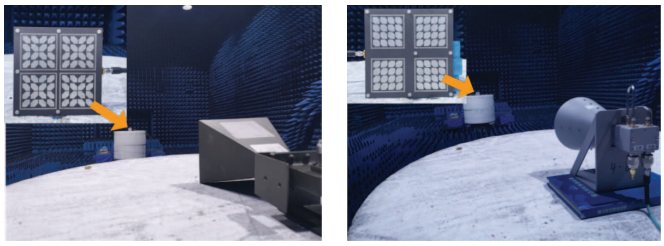


Fig. 10. Photographs of measurement environment.

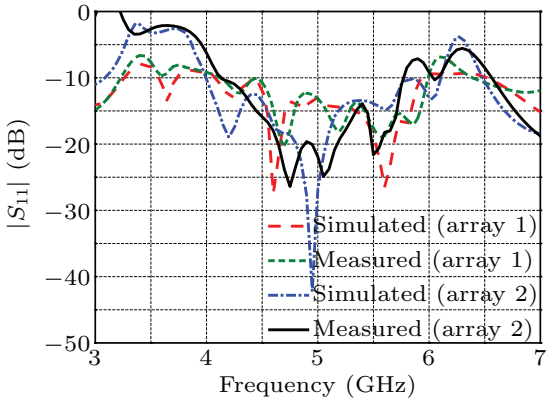


Fig. 11. Simulated and measured curves of *S* parameter *versus* frequency of antenna array.

Figure 12 shows the frequency dependent AR curve of the circularly polarized array, and the simulated operating band that is 1.25 GHz (4.4 GHz–5.65 GHz) while the measured one is 1.3 GHz (4.2 GHz–5.5 GHz). It can be clearly seen that the AR bandwidth is broadened compared with the counterpart in Fig. 4(b). This is credited with the sequential rotation which further verifies the validity of sequential rotation and the designed broadband phase shift network.

The simulated and measured gains of the antenna arrays are plotted in Fig. 13, we can see that the gain of the array is improved by 3 dB due to the forming array. This matches the basic theories of antenna and means that the grating lobe does not appear to affect the antenna performance. The gain variation of the high gain array is 10.4 dBi–14.2 dBi in the operating band and 0.9 dBi in the band of 3.95 GHz–5.75 GHz. The gain variation of the circularly polarized array is 9.1 dBi–12.1 dBi in the operating band and 1 dBi in the band of 4.05 GHz–5.65 GHz. At the same frequency points, the gain of the high gain array is improved by 2 dBi in comparison with that of the circularly polarized array. Furthermore, the simulated gains of the two arrays are similar to the sub arrays, which verifies the validity of the design. The measured results accord well with the simulated results and have high stability.

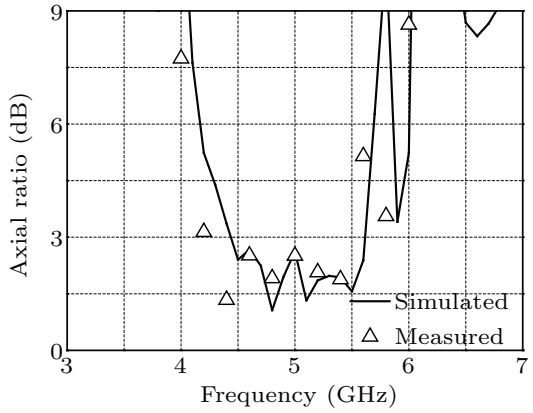


Fig. 12. AR *versus* frequency curve of circularly polarized array.

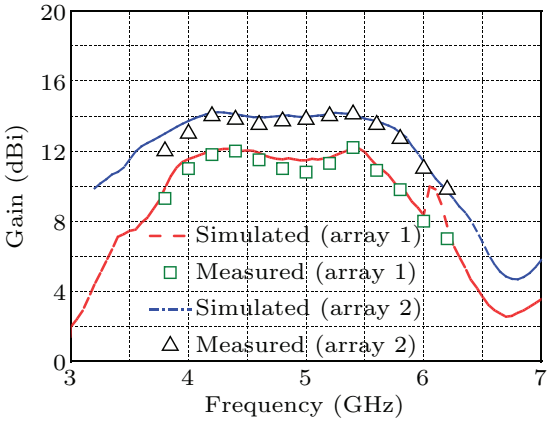


Fig. 13. Simulated and measured gain *versus* frequency of the antenna array.

Figures 14 and 15 show the measured and simulated *E*- and *H*-plane radiation patterns at 5 GHz of the circularly polarized array and high gain array, respectively. It is demonstrated that the simulated results are in good agreement with the measured results, especially those of the main lobe. The difference results from the machining error and the influence caused by the measured environment. The comparisons between other reported designs and the proposed high gain array are listed in Table 1. We can see that in the similar frequency bands, the working bandwidth of the proposed antenna is wider. Furthermore, the gain is further improved and the gain remains steady in the whole operating band due to introduce of novel metasurface structure.

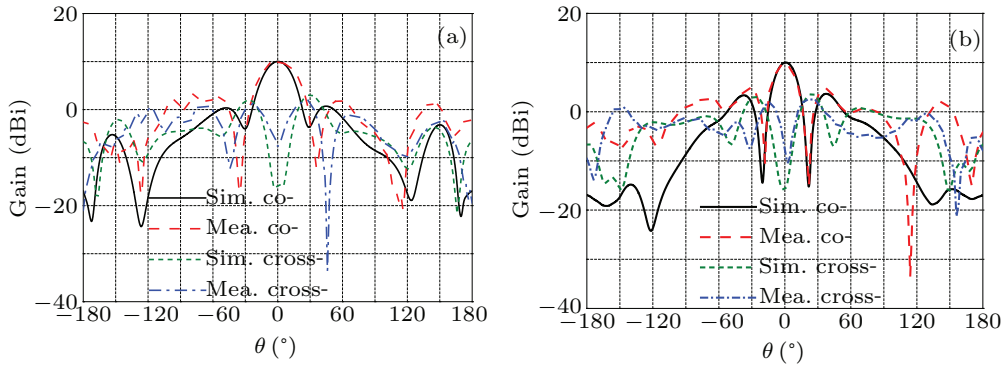


Fig. 14. Simulated (Sim.) and measured (Mea.) E-plane (a) and H-plane (b) radiation patterns of circularly polarized array (5 GHz).

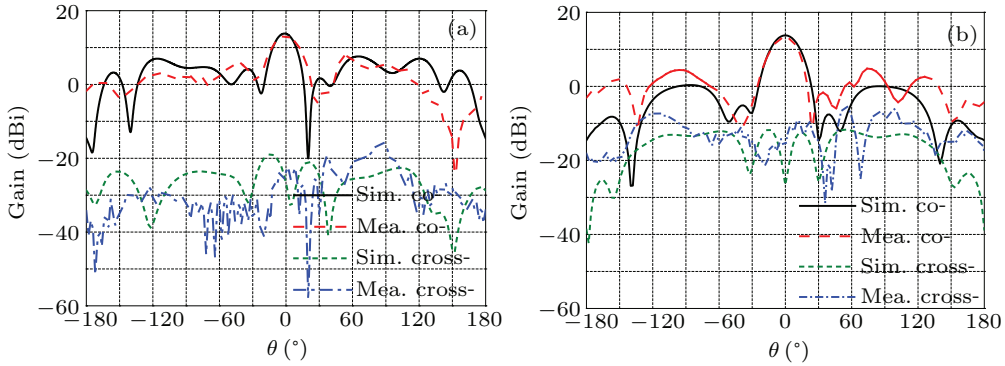


Fig. 15. Simulated and measured E-plane (a) and H-plane (b) radiation patterns of high gain array (5 GHz).

Table 1. Comparison between proposed antenna and other designed antennas in references.

Ref.	Frequency (GHz)	Bandwidth (%)	Peak gain (dBi)	Array	Dimensions (λ_0)
[5]	5.5	31	14.5	2×2	1.78×1.78 ×0.07
[6]	5	28	8.4	2×2	1.58×1.58 ×0.07
[27]	45	32	18.2	4×4	5.1×4.1 ×0.11
[28]	5.8	5.3	10.75	2×2	0.97×0.97 ×0.07
This work	5	42.7	14.2	2×2	2.18×2.18 ×0.06

Note that λ_0 is the wavelength at the lowest resonant frequency.

4. Conclusions

Two substrate integrated waveguide (SIW) cavity metasurface antenna arrays are proposed in this work. By rotating the metasurface element, the circularly polarized antenna and high gain antennas are achieved. Firstly, multi-mode resonance theory is employed to broaden the bandwidth of the slot antenna. Secondly, an SIW cavity composed of 4×4 corner-cut elements is added on the top of the slot antenna to achieve the circular polarization and improve the front-to-back ratio. Thirdly, the metasurface elements are sequentially rotated and a high gain antenna with 2-dBi enhancement on average in the operation band is obtained. And then, two 2×2 antenna arrays are formed. The simulation and measurement results are in good agreement with each other , indicating the efficiency of the design.

Acknowledgement

Project supported by the National Natural Science Foundation of China (Grant No. 61871394).

References

[1] Ding W, Chen Y H and Li Z Y 2014 *Chin. Phys. B* **23** 037301
[2] Tian C, Jiao Y C, Zhao G and Wang H 2018 *IEEE Anten. Wirel. Propag. Lett.* **16** 1561
[3] Wang L J, Chen Q H, Yu F L and Gao X 2018 *Chin. Phys. B* **27** 087802
[4] Nakmouche M F, Allam A M, Fawzy D E and Abdalla M 2021 *Prog. Electromagn. Res. Lett.* **101** 117
[5] Lin F H and Chen Z N 2017 *IEEE Trans. Anten. Propag.* **65** 1706
[6] Nie N S, Yang X S, Chen Z N and Wang B Z 2020 *IEEE Trans. Anten. Propag.* **68** 665
[7] Yu Y Q, Fan Y W and Wang X Y 2020 *Chin. Phys. B* **29** 118402
[8] Liu K Y, Wang G M, Cai T, Li H P and Li T Y 2021 *IEEE Trans. Anten. Propag.* **69** 3349
[9] Xie P, Wang G M, Li H P, Liang J G and Gao X J 2020 *IEEE Trans. Anten. Propag.* **68** 3213
[10] Zhang H L, Hu B J and Zhang X Y 2012 *Chin. Phys. B* **21** 027701

[11] Ta S X and Park I 2017 *IEEE Anten. Wirel. Propag. Lett.* **16** 1932

[12] Wu J, Cheng Y J and Fan Y 2016 *IEEE Trans. Anten. Propag.* **64** 535

[13] Ta S X, Kiem N K and Chien D N 2019 *Prog. Electromagn. Res. C* **97** 57

[14] Yu Z, Shen Z X and Feng Y J 2014 *Chin. Phys. B* **23** 034101

[15] Guan D F, Qian Z P, Zhang Y S and Cai Y 2014 *IEEE Anten. Wirel. Propag. Lett.* **13** 423

[16] Mbaye M, Talbi L, Louati S, Hettak K and Boutayeb H 2022 *Prog. Electromagn. Res. M* **107** 79

[17] Wu G C, Wang G M, Fu X L, Liang J G and Bai W X 2017 *Chin. Phys. B* **26** 024102

[18] Cheng T, Jiang W, Gong S X and Yu Y Q 2019 *IEEE Anten. Wirel. Propag. Lett.* **18** 936

[19] Cai Y, Zhang Y S, Ding C and Qian Z P 2017 *IEEE Trans. Anten. Propag.* **65** 3465

[20] Li T and Chen Z N 2018 *IEEE Trans. Anten. Propag.* **66** 6742

[21] Xie P, Wang G M, Zong B F and Zou X J 2021 *Chin. Phys. B* **30** 084103

[22] Hou H S, Wang G M, Li H P, Guo W L, Li T J and Cai T 2017 *Chin. Phys. B* **26** 057701

[23] Li H P, Wang G M, Cai T, Liang J G and Gao X J 2018 *IEEE Trans. Anten. Propag.* **66** 5121

[24] Li T and Chen Z N 2018 *IEEE Trans. Anten. Propag.* **66** 2862

[25] Li Y B, Li A B, Cu i T J and Sievenpiper D F 2018 *IEEE Trans. Anten. Propag.* **66** 6408

[26] Xu H X, Wang S J, Wang C H, Wang M Z, Wang Y Z and Peng Q 2017 *IEEE Trans. Anten. Propag.* **65** 7378

[27] Li C F, Zhu X W, Liu P F, Yu C and Hong W 2019 *IEEE Anten. Wirel. Propag. Lett.* **18** 1208

[28] Yang W C, Chen S, Che W Q, Xue Q and Meng Q 2018 *IEEE Trans. Anten. Propag.* **66** 4918

[29] Wu T, Chen J and Wu P F 2020 *AEU-Int. J. Electron. Commun.* **127** 153440